International Journal of Pressure Vessels and Piping 87 (2010) 414–423

Contents lists available at ScienceDirect

International Journal of Pressure Vessels and Piping

journal homepage: www.elsevier.com/locate/ijpvp

Shell analysis of thin-walled pipes. Part II – Finite element formulation

Kevin Weicker [a], Raydin Salahifar [b], Magdi Mohareb [b,*]

[a] British Columbia Ministry of Transportation and Infrastructure, Kamloops, BC, Canada V2C 2T3
[b] Department of Civil Engineering, University of Ottawa, Ottawa, ON, Canada K1N 6N5

ARTICLE INFO

Article history:
Received 13 March 2009
Received in revised form
30 March 2010
Accepted 31 March 2010

Keywords:
Shell theory
Pipe
Combined loads
Fourier series
Principle of stationary potential energy
Finite element analysis

ABSTRACT

A finite element formulation is developed for the analysis of thin-walled pipes based on thin shell theory. The formulation starts with a Fourier series solution of the equilibrium equations developed in a companion paper and develops a family of exact shape functions for each mode. The shape functions developed are used in conjunction with the principle of stationary potential energy and yield a finite element that is exact within the assumptions of the underlying shell formulation. The stiffness matrix contribution for each mode n is observed to be fully uncoupled from those based on other modes $m \neq n$. The resulting finite element is shown to be free from discretization errors normally occurring in conventional finite elements. The applicability of the solution is illustrated through examples with various loading cases and boundary conditions. A comparison with other finite element and closed form solutions demonstrates the validity and accuracy of the current finite element.

1. Introduction and scope

In a companion paper [1], the governing equilibrium conditions and possible boundary conditions for thin-walled pipes were developed and solved using a Fourier series solution. A closed form solution was developed for two practical examples. While the solutions developed are exact within the limitations of the assumptions, the solution process was found to be particularly lengthy to conduct by hand. In this context, the present paper attempts to preserve the exactness of the solution while automating it by implementing a finite element solution based on the exact solution of the field equations already developed.

2. Literature review

A comprehensive review on finite element formulations for the analysis of pipes is provided in the series of review papers [2–5]. Most of the formulations were related to pipe bends subjected to specific load patterns. For the most part, the work is applicable to straight pipes (as straight pipes can be conceived as elbows with infinite radius of curvature). A comparative review of strain–displacement relationships in various shell formulations was presented in the companion paper [1].

In all the research discussed below, the kinematic assumptions of the Love–Kirchhoff thin shell theory are adopted. These are (a) straight fibres perpendicular to the middle surface before deformation remain straight and perpendicular to the middle surface after deformation, and (b) the radial normal stress and transverse shear stresses are neglected.

This includes the work of Ohtsubo and Watanabe [6] who developed a finite element as an assembly of ring elements. Their formulation captures shear deformation and warping effects but assumes inextensible hoop strains. The formulation is applicable to both in-plane and out of plane bending. The displacement fields were assumed to have a harmonic distribution in the circumferential direction. In the longitudinal direction, the displacement fields were interpolated using Hermitian polynomials.

Bathe and Almeida [7] developed a four node finite element for the linear analysis of elbows with large bend radii by assuming a cubic Lagrangian interpolation for the tangential and radial displacements over the length of the elbow. Their formulation neither captured warping deformations nor radial expansion. Subsequent improvements included developing interaction effects between elbow elements and straight pipe segments [8] and developing the non-linear capabilities for the element [9].

Militello and Huespe [10] further improved the element by Bathe and Almeida [7] by capturing warping deformations by interpolating the longitudinal displacements with cubic Lagrangian polynomials. They expanded the tangential and radial displacements using a limited number of Fourier series terms.

Another improvement to Bathe and Almeida's element was conducted by Abo-Elkhier [11] who adopted more complete displacement–strain relations in their formulation.

* Corresponding author. Tel.: +1 (613) 562 5800x6130; fax: +1 (613) 563 5173.
E-mail address: mmohareb@uottawa.ca (M. Mohareb).

0308-0161/$ – see front matter © 2010 Elsevier Ltd. All rights reserved.
doi:10.1016/j.ijpvp.2010.03.026

The pipe inextensibility assumption in the radial direction was relaxed in the work of Yan et al. [12] who developed a formulation for plastic limit load of pipe elbows. The remainder of their formulation is consistent with that of Militello and Huespe [10]. The longitudinal, tangential and radial displacements were all expressed as Fourier series in the circumferential direction with cubic Lagrangian interpolation polynomials for the longitudinal displacement and Hermitian polynomials for the tangential and radial displacements.

Karamanos [13] broadened the previous work to model buckling instability of pipes. His work included non-linear elastic effects and investigated the relationship between ovalization and buckling of pipes subjected to constant bending moments. His work was followed up by Karamanos et al. [14] who included the effects of plasticity and internal pressure.

2.1. Expression for the potential energy

The total potential energy $\prod^*$ of the system for a pipe element of length ℓ, mid-surface radius r and thickness t, undergoing displacements u, v and w in the z (longitudinal), ϕ (tangential) and ρ (radial) directions, respectively, under externally applied tractions $q_u(z,\phi)$, $q_v(z,\phi)$, and $q_w(z,\phi)$ acting on the middle surface of the pipe [1] is

$$\begin{aligned}\prod^* = \frac{1}{2}\int_{z=0}^{\ell}\int_{\phi=0}^{2\pi}\Bigg\langle &\frac{Et}{1-\nu^2}\Bigg\{\left(\frac{\partial u}{\partial z}\right)^2+\frac{1}{r^2}\left[w^2+2w\frac{\partial v}{\partial\phi}+\left(\frac{\partial v}{\partial\phi}\right)^2\right]\\ &+2\nu\left(\frac{\partial u}{\partial z}\right)\left(\frac{1}{r}\right)\left(w+\frac{\partial v}{\partial\phi}\right)\Bigg\}+Gt\Bigg[\left(\frac{\partial v}{\partial z}\right)^2+\frac{2}{r}\frac{\partial v}{\partial z}\frac{\partial u}{\partial\phi}\\ &+\frac{1}{r^2}\left(\frac{\partial u}{\partial\phi}\right)^2\Bigg]+\frac{Et^3}{12(1-\nu^2)}\Bigg\{\left(\frac{\partial^2 w}{\partial z^2}\right)^2+\frac{1}{r^4}\Bigg[\left(\frac{\partial^2 w}{\partial\phi^2}\right)^2\\ &-2\left(\frac{\partial^2 w}{\partial\phi^2}\right)\left(\frac{\partial v}{\partial\phi}\right)+\left(\frac{\partial v}{\partial\phi}\right)^2\Bigg]+\frac{2\nu}{r^2}\left(\frac{\partial^2 w}{\partial z^2}\right)\left(\frac{\partial^2 w}{\partial\phi^2}-\frac{\partial v}{\partial\phi}\right)\Bigg\}\\ &+\frac{Gt^3}{3r^2}\Bigg[\left(\frac{\partial^2 w}{\partial z\partial\phi}\right)^2-2\left(\frac{\partial^2 w}{\partial z\partial\phi}\right)\left(\frac{\partial v}{\partial z}\right)+\left(\frac{\partial v}{\partial z}\right)^2\Bigg]\\ &-[q_u(z,\phi)u+q_v(z,\phi)v+q_w(z,\phi)w]\Bigg\rangle r\,\mathrm{d}\phi\,\mathrm{d}z\end{aligned}\tag{1}$$

In Eq. (1), ν is Poisson's ratio, E is Young's Modulus of the pipe material and G is the shear modulus of the pipe material.

2.2. Displacement fields

Consistently with the formulation in the companion paper [1], the mid-surface displacements are expressed as Fourier expansions of the coordinate ϕ as:

$$\begin{aligned}u(z,\phi) &= a_0(z)+\sum_{n=1}^{\alpha}a_n(z)\cos n\phi+\sum_{n=1}^{\alpha}b_n(z)\sin n\phi\\ v(z,\phi) &= c_0(z)+\sum_{n=1}^{\alpha}c_n(z)\cos n\phi+\sum_{n=1}^{\alpha}d_n(z)\sin n\phi\\ w(z,\phi) &= f_0(z)+\sum_{n=1}^{\alpha}f_n(z)\cos n\phi+\sum_{n=1}^{\alpha}g_n(z)\sin n\phi\end{aligned}\tag{2a-c}$$

In Eqs. (2a–c), functions $a_0(z)$, $a_n(z)$, $b_n(z)$, $c_0(z)$, $c_n(z)$, $d_n(z)$, $f_0(z)$, $f_n(z)$ and $g_n(z)$ are displacement functions to be determined from equilibrium considerations. When α is infinite, the series solution converges to the exact solution of the problem within the limitations of the assumptions made. In practicality, the series solution will be truncated as α is chosen as a finite number.

2.3. Formulation of exact shape functions

The closed form solution for the unknown displacement functions $a_0(z),\ldots,g_n(z)$, which satisfy the homogeneous part of the equilibrium conditions, were derived in the companion paper [1] as:

$$\begin{aligned}a_0(z) &= \langle e_0(z)\rangle_{1\times8}^{\mathrm{T}}\{\overline{A}_0\}_{8\times1},\quad c_0(z) = \langle\overline{\overline{C}}_0(z)\rangle_{1\times8}^{\mathrm{T}}\{\overline{A}_0\}_{8\times1},\\ f_0(z) &= \langle\overline{\overline{F}}_0(z)\rangle_{1\times8}^{\mathrm{T}}\{\overline{A}_0\}_{8\times1}\\ a_n(z) &= \langle\overline{\overline{A}}_n(z)\rangle_{1\times8}^{\mathrm{T}}\{\overline{F}_n\}_{8\times1},\quad d_n(z) = \langle\overline{\overline{D}}_n(z)\rangle_{1\times8}^{\mathrm{T}}\{\overline{F}_n\}_{8\times1},\\ f_n(z) &= \langle e_n(z)\rangle_{1\times8}^{\mathrm{T}}\{\overline{F}_n\}_{8\times1}\\ b_n(z) &= \langle\overline{\overline{A}}_n(z)\rangle_{1\times8}^{\mathrm{T}}\{\overline{G}_n\}_{8\times1},\quad c_n(z) = -\langle\overline{\overline{D}}_n(z)\rangle_{1\times8}^{\mathrm{T}}\{\overline{G}_n\}_{8\times1},\\ g_n(z) &= \langle e_n(z)\rangle_{1\times8}^{\mathrm{T}}\{\overline{G}_n\}_{8\times1}\end{aligned}\tag{3a-i}$$

$$n = 1,..\alpha$$

In Eqs. (3a–i), vectors $\{\overline{A}_0\}_{8\times1}$, $\{\overline{F}_n\}_{8\times1}$, $\{\overline{G}_n\}_{8\times1}$ are

$$\begin{aligned}\langle\overline{A}_0\rangle_{1\times8}^{T} &= \langle\,\overline{A}_{0,1}\ \ \overline{A}_{0,2}\ \ \overline{A}_{0,3}\ \ \overline{A}_{0,4}\ \ \overline{A}_{0,5}\ \ \overline{A}_{0,6}\ \ \overline{A}_{0,7}\ \ \overline{A}_{0,8}\,\rangle^T\\ \langle\overline{F}_n\rangle_{1\times8}^{T} &= \langle\,\overline{F}_{n,1}\ \ \overline{F}_{n,2}\ \ \overline{F}_{n,3}\ \ \overline{F}_{n,4}\ \ \overline{F}_{n,5}\ \ \overline{F}_{n,6}\ \ \overline{F}_{n,7}\ \ \overline{F}_{n,8}\,\rangle^T\\ \langle\overline{G}_n\rangle_{1\times8}^{T} &= \langle\,\overline{G}_{n,1}\ \ \overline{G}_{n,2}\ \ \overline{G}_{n,3}\ \ \overline{G}_{n,4}\ \ \overline{G}_{n,5}\ \ \overline{G}_{n,6}\ \ \overline{G}_{n,7}\ \ \overline{G}_{n,8}\,\rangle^T\end{aligned}\tag{4a-c}$$

They consist of integration constants to be determined from the boundary conditions of the problem, and the function vectors $\langle e_0(z)\rangle_{1\times8}^{\mathrm{T}}$, $\langle\overline{\overline{C}}_0(z)\rangle_{1\times8}^{\mathrm{T}}$, $\langle\overline{\overline{F}}_0(z)\rangle_{1\times8}^{\mathrm{T}}$, $\langle\overline{\overline{A}}_n(z)\rangle_{1\times8}^{\mathrm{T}}$, $\langle\overline{\overline{D}}_n(z)\rangle_{1\times8}^{\mathrm{T}}$, $\langle e_n(z)\rangle_{1\times8}^{\mathrm{T}}$ as obtained in [1] are summarized in Appendix A. We recall that the solution fields for the equilibrium equations as developed in [1] were observed to fully uncouple the contribution of mode n from that of mode $m\neq n$, a feature that is exploited in the present formulation.

In the present paper, rather than assuming conventional polynomial functions, we start with the exact solution of the displacement fields (Eqs. (3a–i)) to formulate the exact shape functions. This is done by expressing the vectors of integration constants $\{\overline{A}_0\}_{8\times1}$, $\{\overline{F}_n\}_{8\times1}$, $\{\overline{G}_n\}_{8\times1}$ in terms of the nodal displacements $\langle\Delta_0\rangle_{1\times8}^{\mathrm{T}}$, $\langle\Delta_{n,1}\rangle_{1\times8}^{\mathrm{T}}$, $\langle\Delta_{n,2}\rangle_{1\times8}^{\mathrm{T}}$ defined as

$$\begin{aligned}\langle\Delta_0\rangle_{1\times8}^{\mathrm{T}} &= \langle a_0(0)\ \ c_0(0)\ \ f_0(0)\ \ f'_0(0)\ \ a_0(\ell)\ \ c_0(\ell)\ \ f_0(\ell)\ \ f'_0(\ell)\rangle^{\mathrm{T}}\\ \langle\Delta_{n,1}\rangle_{1\times8}^{\mathrm{T}} &= \langle a_n(0)\ \ c_n(0)\ \ f_n(0)\ \ f'_n(0)\ \ a_n(\ell)\ \ c_n(\ell)\ \ f_n(\ell)\ \ f'_n(\ell)\rangle^{\mathrm{T}}\\ \langle\Delta_{n,2}\rangle_{1\times8}^{\mathrm{T}} &= \langle b_n(0)\ \ d_n(0)\ \ g_n(0)\ \ g'_n(0)\ \ b_n(\ell)\ \ d_n(\ell)\ \ g_n(\ell)\ \ g'_n(\ell)\rangle^{\mathrm{T}}\end{aligned}\tag{5a-c}$$

through

$$\begin{aligned}\{\Delta_0\}_{8\times1} &= [L_0]_{8\times8}\{\overline{A}_0\}_{8\times1}\\ \{\Delta_{n,1}\}_{8\times1} &= [L_{n,1}]_{8\times8}\{\overline{F}_n\}_{8\times1}\\ \{\Delta_{n,2}\}_{8\times1} &= [L_{n,2}]_{8\times8}\{\overline{G}_n\}_{8\times1}\end{aligned}\tag{6a-c}$$

in which matrices $[L_0]_{8\times8}$, $[L_{n,1}]_{8\times8}$ and $[L_{n,2}]_{8\times8}$ are defined in Appendix B. Eqs. (6a–c) are solved for the vectors of integration constants yielding

$$\begin{aligned}\{\overline{A}_0\}_{8\times1} &= [L_0]_{8\times8}^{-1}\{\Delta_0\}_{8\times1}\\ \{\overline{F}_n\}_{8\times1} &= [L_{n,1}]_{8\times8}^{-1}\{\Delta_{n,1}\}_{8\times1}\\ \{\overline{G}_n\}_{8\times1} &= [L_{n,2}]_{8\times8}^{-1}\{\Delta_{n,2}\}_{8\times1}\end{aligned}\tag{7a-c}$$

From Eqs. (7a–c), by substituting into Eqs. (3a–i), one obtains

$$a_0(z) = \langle \bar{e}_0(z)\rangle^{\mathrm{T}}_{1\times 8}[L_0]^{-1}_{8\times 8}\{\Delta_0\}_{8\times 1} = \langle N_{A,0}(z)\rangle^{\mathrm{T}}_{1\times 8}\{\Delta_0\}_{8\times 1}$$
$$c_0(z) = \langle \bar{\bar{C}}_0(z)\rangle^{\mathrm{T}}_{1\times 8}[L_0]^{-1}_{8\times 8}\{\Delta_0\}_{8\times 1} = \langle N_{C,0}(z)\rangle^{\mathrm{T}}_{1\times 8}\{\Delta_0\}_{8\times 1}$$
$$f_0(z) = \langle \bar{\bar{F}}_0(z)\rangle^{\mathrm{T}}_{1\times 8}[L_0]^{-1}_{8\times 8}\{\Delta_0\}_{8\times 1} = \langle N_{F,0}(z)\rangle^{\mathrm{T}}_{1\times 8}\{\Delta_0\}_{8\times 1}$$
$$a_n(z) = \langle \bar{\bar{A}}_n(z)\rangle^{\mathrm{T}}_{1\times 8}[L_{n,1}]^{-1}_{8\times 8}\{\Delta_{n,1}\}_{8\times 1} = \langle N_{A,n}(z)\rangle^{\mathrm{T}}_{1\times 8}\{\Delta_{n,1}\}_{8\times 1}$$
$$d_n(z) = \langle \bar{\bar{D}}_n(z)\rangle^{\mathrm{T}}_{1\times 8}[L_{n,1}]^{-1}_{8\times 8}\{\Delta_{n,1}\}_{8\times 1} = \langle N_{D,n}(z)\rangle^{\mathrm{T}}_{1\times 8}\{\Delta_{n,1}\}_{8\times 1}$$
$$f_n(z) = \langle \bar{e}_n(z)\rangle^{\mathrm{T}}_{1\times 8}[L_{n,1}]^{-1}_{8\times 8}\{\Delta_{n,1}\}_{8\times 1} = \langle N_{F,n}(z)\rangle^{\mathrm{T}}_{1\times 8}\{\Delta_{n,1}\}_{8\times 1}$$
$$b_n(z) = \langle \bar{\bar{A}}_n(z)\rangle^{\mathrm{T}}_{1\times 8}[L_{n,2}]^{-1}_{8\times 8}\{\Delta_{n,2}\}_{8\times 1} = \langle N_{B,n}(z)\rangle^{\mathrm{T}}_{1\times 8}\{\Delta_{n,2}\}_{8\times 1}$$
$$c_n(z) = -\langle \bar{\bar{D}}_n(z)\rangle^{\mathrm{T}}_{1\times 8}[L_{n,2}]^{-1}_{8\times 8}\{\Delta_{n,2}\}_{8\times 1} = \langle N_{C,n}(z)\rangle^{\mathrm{T}}_{1\times 8}\{\Delta_{n,2}\}_{8\times 1}$$
$$g_n(z) = \langle \bar{e}_n(z)\rangle^{\mathrm{T}}_{1\times 8}[L_{n,2}]^{-1}_{8\times 8}\{\Delta_{n,2}\}_{8\times 1} = \langle N_{G,n}(z)\rangle^{\mathrm{T}}_{1\times 8}\{\Delta_{n,2}\}_{8\times 1} \quad (8\mathrm{a}-\mathrm{i})$$

It is noted that the series of interpolation functions provided in Eqs. (8a–i) exactly satisfy the homogeneous part of the equilibrium equations, i.e., the shape functions are exact. From Eqs. (8a–i), substituting into Eq. (2), one obtains

$$u(z,\phi) = \langle N_{A,0}(z)\rangle^{\mathrm{T}}_{1\times 8}\{\Delta_0\}_{8\times 1} + \sum_{n=1}^{\alpha}\langle N_{A,n}(z)\rangle^{\mathrm{T}}_{1\times 8}\{\Delta_{n,1}\}_{8\times 1}\cos n\phi + \sum_{n=1}^{\alpha}\langle N_{B,n}(z)\rangle^{\mathrm{T}}_{1\times 8}\{\Delta_{n,2}\}_{8\times 1}\sin n\phi$$
$$v(z,\phi) = \langle N_{C,0}(z)\rangle^{\mathrm{T}}_{1\times 8}\{\Delta_0\}_{8\times 1} + \sum_{n=1}^{\alpha}\langle N_{D,n}(z)\rangle^{\mathrm{T}}_{1\times 8}\{\Delta_{n,1}\}_{8\times 1}\sin n\phi + \sum_{n=1}^{\alpha}\langle N_{C,n}(z)\rangle^{\mathrm{T}}_{1\times 8}\{\Delta_{n,2}\}_{8\times 1}\cos n\phi$$
$$w(z,\phi) = \langle N_{F,0}(z)\rangle^{\mathrm{T}}_{1\times 8}\{\Delta_0\}_{8\times 1} + \sum_{n=1}^{\alpha}\langle N_{F,n}(z)\rangle^{\mathrm{T}}_{1\times 8}\{\Delta_{n,1}\}_{8\times 1}\cos n\phi + \sum_{n=1}^{\alpha}\langle N_{G,n}(z)\rangle^{\mathrm{T}}_{1\times 8}\{\Delta_{n,2}\}_{8\times 1}\sin n\phi \quad (9\mathrm{a}-\mathrm{c})$$

It is observed that the displacement fields in Eqs. (9a–c) $u(z,\phi), v(z,\phi), w(z,\phi)$ happen to be functions of the same 8×1 nodal displacement vectors $\{\Delta_0\},\{\Delta_{n,1}\},\{\Delta_{n,2}\}$. This contrasts with other solutions based on polynomial interpolation functions ([6,7,10,12], etc.) in which the displacement fields are expressed in terms of subsets of the nodal displacements $\{\Delta_0\},\{\Delta_{n,1}\},\{\Delta_{n,2}\}$. For instance, when using linear interpolation functions $\langle N(z)\rangle^{\mathrm{T}}_{1\times 2} = \langle (z/\ell) \quad (1-z/\ell)\rangle^{T}$ in expressing field $u(z,\phi)$ in terms of the nodal displacements $\langle \overline{\Delta_{n,1}}\rangle^{T} = \langle a_n(0), a_n(\ell)\rangle^{T}_{1\times 2}$, conventional solutions use the simpler form

$$u(z,\phi) = \langle N(z)\rangle^{\mathrm{T}}_{1\times 2}\{\overline{\Delta_0}\}_{2\times 1} + \sum_{n=1}^{\alpha}\langle N(z)\rangle^{\mathrm{T}}_{1\times 2}\left\{\overline{\Delta_{n,1}}\right\}_{2\times 1}\cos n\phi + \sum_{n=1}^{\alpha}\langle N(z)\rangle^{\mathrm{T}}_{1\times 2}\left\{\overline{\Delta_{n,2}}\right\}_{2\times 1}\sin n\phi \quad (10)$$

which assumes the displacements $u(z,\phi)$ as a function only of $a_n(0), a_n(\ell)$ and thus neglects the coupling between $u(z,\phi)$ and remaining degrees of freedom $c_n(0), f_n(0), f'_n(0), c_n(\ell), f_n(\ell), f'_n(\ell)$. In this respect, the present formulation captures this coupling with implications on the accuracy of the solution as will later be illustrated in the examples.

2.4. Formulation of discrete equilibrium conditions

Substituting the expressions for the displacements (Eqs. (9a–c)) into the expression for the total potential energy (Eq. (1)), performing the integral over the length, and setting the variation of the total potential energy to zero, one recovers the discretised equilibrium equations of the problem.

$$\begin{aligned}\delta\prod{}^{*} &= \delta U - \delta V \\ &= \langle\delta\Delta_0\rangle^{\mathrm{T}}_{1\times 8}\left([K_0]_{8\times 8}\{\Delta_0\}_{8\times 1} - \{Q_0\}_{8\times 1}\right) + \sum_{n=1}^{\alpha}\langle\delta\Delta_{n,1}\rangle^{\mathrm{T}}_{1\times 8}\left([K_{n,1}]_{8\times 8}\{\Delta_{n,1}\}_{8\times 1} - \{Q_{n,1}\}_{8\times 1}\right) + \sum_{n=1}^{\alpha}\langle\delta\Delta_{n,2}\rangle^{\mathrm{T}}_{1\times 8}\left([K_{n,2}]_{8\times 8}\{\Delta_{n,2}\}_{8\times 1} - \{Q_{n,2}\}_{8\times 1}\right) = 0 \end{aligned} \quad (11)$$

where matrices and vectors $[K_0]_{8\times 8}$, $[K_{n,1}]_{8\times 8}$, $[K_{n,2}]_{8\times 8}$ and $\{Q_0\}_{8\times 1}$, $\{Q_{n,1}\}_{8\times 1}$, $\{Q_{n,2}\}_{8\times 1}$, respectively, are defined in Appendix C.

3. Implementation

For a single element and for $\alpha+1$ modes, the above algorithm yields $(2\alpha+1)$ independent systems of equations, each having 8 degrees of freedom of the form

$$\begin{aligned}&[K_0]_{8\times 8}\{\Delta_0\}_{8\times 1} = \{Q_0\}_{8\times 1} \\ &[K_{n,1}]_{8\times 8}\{\Delta_{n,1}\}_{8\times 1} = \{Q_{n,1}\}_{8\times 1} \quad ,n = 1\ldots\alpha \\ &[K_{n,2}]_{8\times 8}\{\Delta_{n,2}\}_{8\times 1} = \{Q_{n,2}\}_{8\times 1} \quad ,n = 1\ldots\alpha\end{aligned} \quad (12\mathrm{a}-\mathrm{c})$$

The total number of degrees of freedom for a single element is $(16\alpha+8)$. For a pipeline system consisting of k nodes, one obtains $(2\alpha+1)$ of independent systems of equations, each having $4k$ degrees of freedom, taking the form

$$\begin{aligned}&[K_{S0}]_{4k\times 4k}\{\Delta_{S0}\}_{4k\times 1} = \{Q_{S0}\}_{4k\times 1} \\ &[K_{Sn,1}]_{4k\times 4k}\{\Delta_{Sn,1}\}_{4k\times 1} = \{Q_{Sn,1}\}_{4k\times 1}, \quad n = 1\ldots\alpha \\ &[K_{Sn,2}]_{4k\times 4k}\{\Delta_{Sn,2}\}_{4k\times 1} = \{Q_{Sn,2}\}_{4k\times 1}, \quad n = 1\ldots\alpha\end{aligned} \quad (13\mathrm{a}-\mathrm{c})$$

in which the stiffness matrices and vectors $[K_{S0}]_{4k\times 4k}$, $[K_{Sn,1}]_{4k\times 4k}$, $[K_{Sn,2}]_{4k\times 4k}$, $\{Q_{S0,1}\}_{4k\times 1}$, $\{Q_{Sn,1}\}_{4k\times 1}$, $\{Q_{Sn,2}\}_{4k\times 1}$ are obtained through the conventional finite element assembly technique of the element contributions $[K_0]_{8\times 8}$, $[K_{n,1}]_{8\times 8}$, $[K_{n,2}]_{8\times 8}$, $\{Q_0\}_{8\times 1}$, $\{Q_{n,1}\}_{8\times 1}$, $\{Q_{n,2}\}_{8\times 1}$, respectively. The total number of degrees of freedom for the whole structure is $(8\alpha k+4k)$. In most practical problems (such the four examples in the present paper), the system of $(2\alpha+1)$ equations (Eq. (12)) remain uncoupled after imposing the boundary conditions of the problem. Thus, the solution of the $(8\alpha k+4k)$ unknowns simplifies to the solution of $(2\alpha+1)$ separate systems of $4k\times 4k$ equations, each. In large problem sizes, this has a clear computational advantage. The above formulation was implemented under a C++ program [15].

4. Examples

4.1. Example 1: cantilever pipe subject to point load

Example 1 in the companion paper [1] is solved again in the present paper using the finite element solution developed in the present paper. A steel cantilever (Young Modulus $E = 200{,}000$ MPa, Poisson's Ratio $\nu = 0.3$, Shear Modulus $G = E/2(1+\mu) = 76{,}925$ MPa) with a pipe cross-section with radius $r = 200$ mm , thickness $t = 6$ mm and span $\ell = 4$ m is subject to a downward vertical point load $p = 16$ kN acting at the top fibre of the cross-section.

4.1.1. Solution

A solution for the problem is conducted under the present FEA formulation using a single finite element and seven modes ($\alpha = 6$). For the downward point load P applied at $z = \ell$ and $\phi = \pi/2$, the traction functions are $q_u(z,\phi) = 0$, $q_v(z,\phi) = 0$, and $q_w(z,\phi) = -P\delta(z-\ell)\delta(\phi-\pi/2)$ in which δ is the Dirac Delta Function. By substituting into Eqs. (C.4)–(C.6), one obtains $\{Q_0\}_{8\times 1} =$

$-P\{N_{F,0}(\ell)\}_{8\times1}$, $\{Q_{n,1}\}_{8\times1} = -P\{N_{F,n}(\ell)\}_{8\times1}\cos(n\pi/2)$, and $\{Q_{n,2}\}_{8\times1} = -P\{N_{G,n}(\ell)\}_{8\times1}\sin(n\pi/2)$.

4.1.2. Comparison of displacements

The horizontal and vertical displacements for a point at the top extreme fibre, a point at pipe mid-height, and a point at the bottom fibre, all located at the free end were determined from the present FEA formulation and were found to exactly match those based on the analytical solution in the companion paper [1].

A three-dimensional plot of the displacements predicted by the present model for four modes ($\alpha = 3$) and seven modes ($\alpha = 6$) and as predicted by the ABAQUS shell model (with 16,480 degrees of freedom) are depicted in Fig. 1. The displacement fields is magnified by a factor of 24. A comparison of the solution ($\alpha = 3$) and ($\alpha = 6$) show a reasonable agreement indicating that very good results can be obtained with only a few modes (as little as four modes). Also, the solution for ($\alpha = 6$) and ABAQUS results illustrate the ability of the present model to capture the deformational behaviour of the pipe with far less degrees of freedom (112 in the present solution versus 16,480 in the Abaqus shell solution).

The problem was solved again for a radial point load $P = 16$ kN acting at an angle $\phi = 7\,\pi/8$ to the horizontal, rather than vertically. As expected, the displacements obtained were found to exactly match those based on the first solution after the proper transformations were performed [15].

A second analysis for the problem was conducted with two elements of different length as well as with five elements of equal length. In both cases, the displacements at the free end of the cantilever were found identical to five significant digits, to those based on only a single element. These results illustrate that refining the finite element mesh by using a larger number of smaller elements does not increase the accuracy of the analysis and thus is shown to be unnecessary. This is a natural outcome of the fact that the shape functions of the element exactly satisfy the homogeneous form of the equilibrium conditions. In previous finite element formulations ([6,7,10,12], etc.), the shape functions were interpolated with polynomial functions. With such interpolations, refining the finite element mesh produces results that are more accurate. In the current study, given that the shape functions assumed are exact, mesh refinements are unnecessary.

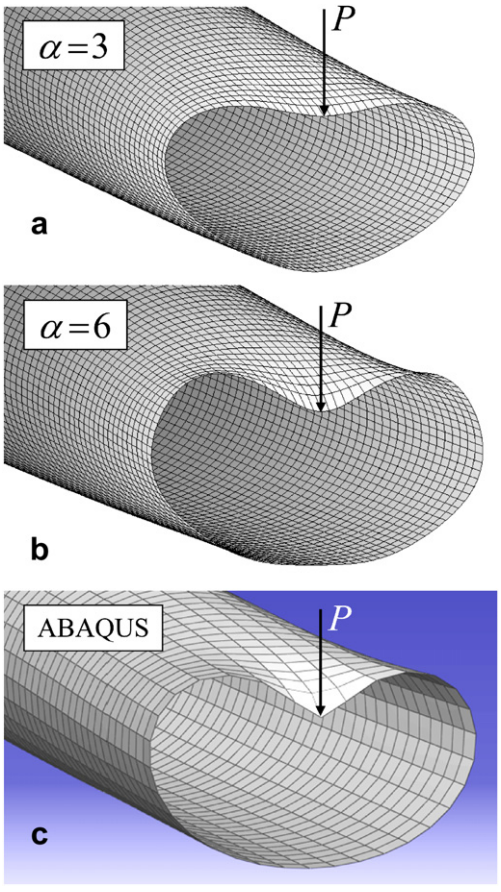

Fig. 1. Deformed configuration under a point load P based on current study with (a) four modes, (b) seven modes, and (c) Abaqus shell model with 3264 elements.

4.1.3. Stresses

The longitudinal stress $\sigma_z(z,\phi,\xi)$ is expressed in terms of the longitudinal strain $\varepsilon_z(z,\phi,\xi)$ and circumferential strain $\varepsilon_\phi(z,\phi,\xi)$ through the generalized Hookes law as $\sigma_z(z,\phi,\xi) = E[\varepsilon_z(z,\phi,\xi) + \nu\varepsilon_\phi(z,\phi,\xi)]/(1-\nu^2)$ in which the longitudinal strain $\varepsilon_z(z,\phi,\xi) = \bar{\varepsilon}_z(z,\phi) - \xi\kappa_z(z,\phi)$ and the circumferential strain $\varepsilon_\phi(z,\phi,\xi) = \bar{\varepsilon}_\phi(z,\phi) - \xi\kappa_\phi(z,\phi)$ are the sum of the respective membrane and bending strains. At the pipe middle surface, $\xi = 0$, the bending strain components vanish and one has $\varepsilon_z(z,\phi,\xi=0) = \bar{\varepsilon}_z(z,\phi) = \partial u/\partial z$ and $\varepsilon_\phi(z,\phi,\xi=0) = \bar{\varepsilon}_\phi(z,\phi) \approx (w/r + \partial v/r\partial\phi)$. This allows expressing the longitudinal stress in terms of the displacement fields as $\sigma_z(z,\phi,\xi=0) = E[\partial u/\partial z + (\nu/r)(w+\partial v/\partial\phi)]/(1-\nu^2)$. From Eq. (9a–c), one obtains

$$\begin{aligned}\sigma_z(z,\phi,\xi=0) = {} & \frac{E}{1-\nu^2}\left(\langle N'_{A,0}(z)\rangle^{\mathrm{T}}_{1\times8} + \frac{\nu}{r}\langle N_{F,0}(z)\rangle^{\mathrm{T}}_{1\times8}\right)\{\Delta_0\}_{8\times1} \\ & + \sum_{n=1}^{\alpha}\frac{E\cos n\phi}{1-\nu^2}\left(\langle N'_{A,n}(z)\rangle^{\mathrm{T}}_{1\times8} + \frac{n\nu}{r}\langle N_{D,n}(z)\rangle^{\mathrm{T}}_{1\times8}\right. \\ & \left. + \frac{\nu}{r}\langle N_{F,n}(z)\rangle^{\mathrm{T}}_{1\times8}\right)\{\Delta_{n,1}\}_{8\times1} + \sum_{n=1}^{\alpha}\frac{E\sin n\phi}{1-\nu^2}\left(\langle N'_{B,n}(z)\rangle^{\mathrm{T}}_{1\times8}\right. \\ & \left. - \frac{n\nu}{r}\langle N_{C,n}(z)\rangle^{\mathrm{T}}_{1\times8} + \frac{\nu}{r}\langle N_{G,n}(z)\rangle^{\mathrm{T}}_{1\times8}\right)\{\Delta_{n,2}\}_{8\times1} \end{aligned} \quad (14)$$

The longitudinal stress for the topmost generator at ($\phi = \pi/2$) on the pipe middle surface based on Eq. 14. The stress contributions from each mode $n = 0$ to $n = 6$ were combined to obtain the total stress. The stress contribution from each mode, the total stress based on all modes, and the longitudinal stress as determined by ABAQUS S4R shell finite element analysis are shown in Fig. 2. Note that the stress contribution for mode $n = 0$ is negligible (<0.7 MPa) and it is not included in Fig. 2.

From Fig. 2 it is apparent that the longitudinal stresses predicted by the current method closely match those determined by the shell finite element. Of particular note is that the current method successfully captures the local stress increase near the applied point load at $z = \ell$. The stress contributions from the higher Fourier modes are responsible for capturing this localized stress while the lower modes, especially mode $n = 1$ captures the stress variation along the remainder of the length of the pipe.

The longitudinal stress at the topmost generator can be determined from the traditional Euler-Bernoulli beam theory as $\sigma = M/S$, where M is the bending moment in the pipe and S is the elastic modulus of the pipe cross-section. The longitudinal stress at Point A predicted by the Euler–Bernoulli beam theory is also depicted in Fig. 2. The Euler–Bernoulli beam theory closely approximates the results of mode $n = 1$ in the current method. This is evidenced by the comparison of both sets of results in the figure.

4.2. Example 2: cantilever pipe under self-weight

The example of a cantilever beam subjected to its self-weight that was analytically solved in the companion paper [1] is solved again using the finite element formulation developed in the present

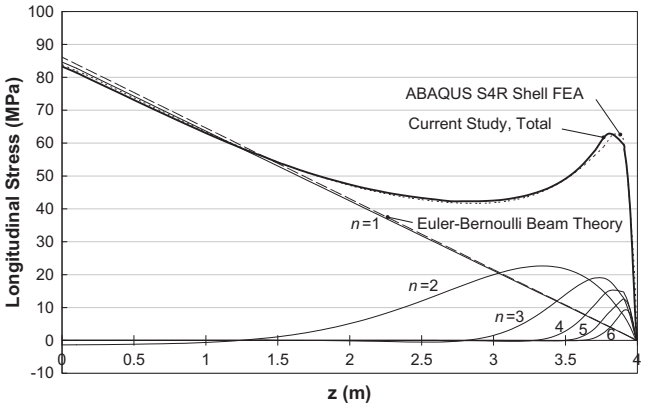

Fig. 2. Longitudinal stress along the topmost generator of the pipe.

study. Material properties of the pipe are: $\ell = 4$ m, $t = 6$ mm, $r = 200$ mm, $\nu = 0.3$, $E = 200{,}000$ MPa and $G = E/2(1+\nu) = 76,925$ MPa.

The load due to the self-weight of a pipe, expressed as $q = t\gamma_s$, acts as vertical traction applied to the entire body of the element. By considering an infinitesimal piece of the pipe with volume $t(r\mathrm{d}\phi)(\mathrm{d}z)$, the load functions in each of the longitudinal, tangential and radial directions are given as $q_u(z,\phi) = 0$, $q_v(z,\phi) = -t\gamma_s\cos\phi$, and $q_w(z,\phi) = -t\gamma_s\sin\phi$. The integrals in Eqs. (C.4)–(C.6) are performed with respect to ϕ leading to

$$\{Q_0\}_{8\times1} = \{0\}_{8\times1}; \quad n = 0$$

$$\{Q_{1,1}\}_{8\times1} = \{0\}_{8\times1}, \ \{Q_{1,2}\}_{8\times1} = -\pi t\gamma_s r \int_{z=0}^{\ell} \{N_{C,1}(z)\}_{8\times1} + \{N_{G,1}(z)\}_{8\times1}\mathrm{d}z; \quad n = 1$$

$$\{Q_{n,1}\}_{8\times1} = \{Q_{n,2}\}_{8\times1} = \{0\}_{8\times1}; \quad n \geq 2 \qquad (15a-e)$$

Thus, the only non-zero nodal displacement contributions come from the solving the system $[K_{1,2}]_{8\times8}\{\Delta_{1,2}\}_{8\times1} = -\pi t\gamma_s r \int_{z=0}^{\ell}\{N_{C,1}(z)\}_{8\times1} + \{N_{G,1}(z)\}_{8\times1}\mathrm{d}z$. The obtained results were observed to exactly match those based on the closed form solution in the companion paper [1].

4.3. Example 3: cantilever pipe subject torque applied at tip

In this example, the pipe in Example 1 is subjected to a twisting moment $T = 10$ kN.m assumed to act as uniform tangential stresses at the end $z = \ell$. The corresponding tractions are $q_u(z,\phi) = 0$, $q_v(z,\phi) = (T/2\pi r^2)\delta(z-\ell)$, and $q_w(z,\phi) = 0$. By substituting into Eqs. (C.4)–(C.6), one obtains, $\{Q_0\}_{8\times1} = (T/r)\{N_{C,0}(\ell)\}_{8\times1}$, $\{Q_{n,1}\}_{8\times1} = \{0\}_{8\times1}$, and $\{Q_{n,2}\}_{8\times1} = \{0\}_{8\times1}$ for $n \geq 1$. The only non-zero displacements $\{\Delta_0\}_{8\times1}$ are obtained from solving the equation $[K_0]_{8\times8}\{\Delta_0\}_{8\times1} - (T/r)\{N_{C,0}(\ell)\}_{8\times1} = \{0\}_{8\times1}$.

For the axi-symmetric loading applied, the resulting tangential displacement is the same for all points on the middle surface. The value of the tangential displacement $v(\ell,\phi) = 0.1103$ mm which corresponds to an angle of twist of $\theta = v(\ell,\phi)/r = 0.1103\ \mathrm{mm}/150\ \mathrm{mm} = 735.3\times10^{-6}$ rad. From the theory of mechanics of materials, the angle of twist at the free end of the cantilever is $\theta_{\mathrm{Theory}} = T\ell/(2\pi Gr^3t) = 735.7\times10^{-6}$ rad, which is nearly identical to the one based on the present formulation.

4.4. Example 4: example with two elements

This example considers a pipe consisting of two segments with different thicknesses. The pipe configuration is shown in Figure 3.

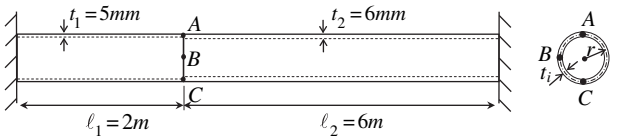

Fig. 3. Multi element pipe.

Both segments of the pipe have $r = 200$ mm, $\nu = 0.3$, $E = 200{,}000$ MPa and $G = \mathrm{E}/2(1+\nu) = 76{,}925$ MPa. While the thickness of the left section is $t_1 = 5$ mm, that of the right segment is $t_2 = 6$ mm.

Two elements are enough to model the two different thicknesses while exactly capturing the exact nodal displacements of the problem (within the limitations of the formulation). The pipe is assumed to be filled with highly pressurized fluid of density $\gamma_w = 10\ \mathrm{kN/m^3}$. The pipe loading consists of internal pressure, $p = 1000$ kPa, self-weight of the fluid, and self weight of the pipe (density $\gamma_s = 78\ \mathrm{kN/m^3}$). Both the internal pressure and the weight of the fluid induce traction components only in the radial direction. From Figure 4, the expressions for the tractions due to the self weight of the fluid and the pressure are $q_{u,1}(z,\phi) = 0$, $q_{v,1}(z,\phi) = 0$, and $q_{w,1}(z,\phi) = -\gamma_w r(\sin\phi - 1) + p$.

The traction expressions for the self-weight of the pipe, $q_{u,2}$, $q_{v,2}$, and $q_{w,2}$ are identical to those of Example 2 (i.e., $q_{u,2}(z,\phi) = 0$, $q_{v,2}(z,\phi) = -t_i\gamma_s\cos\phi$, and $q_{w,2}(z,\phi) = -t_i\gamma_s\sin\phi$) where t_1 and t_2 are the thicknesses of the left and right segments, respectively.

The total tractions for the problem are obtained by adding the contributions of the pressurized fluid and the self-weight of the pipe, which yields $q_u(z,\phi) = 0$, $q_v(z,\phi) = -t_i\gamma_s\cos\phi$, and $q_w(z,\phi) = -\gamma_w r(\sin\phi - 1) + p - t_i\gamma_s\sin\phi$.

By substituting the expressions for tractions q_u, q_v, and q_w into Eqs. (C.4)–(C.6), one obtains the following energy equivalent nodal load vectors

$$\{Q_0\}_{8\times1} = 2\pi r(\gamma_w r + p)\int_{z=0}^{\ell_i}\{N_{F,0}(z)\}_{8\times1}\mathrm{d}z$$

$$\{Q_{1,1}\}_{8\times1} = \{0\}_{8\times1}, \{Q_{1,2}\}_{8\times1,i} = -\pi r t_e\gamma_s\int_{z=0}^{\ell_i}\{N_{C,1}(z)\}_{8\times1}\mathrm{d}z - \pi r(\gamma_w r + t_i\gamma_s)\int_{z=0}^{\ell_i}\{N_{G,1}(z)\}_{8\times1}\mathrm{d}z$$

$$\{Q_{n,1}\}_{8\times1} = \{Q_{n,2}\}_{8\times1} = \{0\}_{8\times1} \quad ;\text{for } n \geq 2 \qquad (16a-e)$$

in which subscripts $i = 1,2$ denote the left and right elements respectively. The total vertical, lateral (horizontal) and longitudinal displacements for Points A, B and C at the intersection of the two elements in the pipe (see Fig. 3) are summarized and compared to the results of the ABAQUS S4R shell finite element analysis in Table 1. In the table, a positive value for the vertical displacement indicates downward movement while a positive value for the longitudinal displacement indicates a displacement along the positive direction of the z axis.

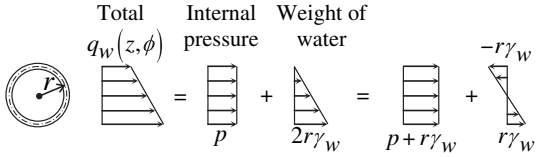

Fig. 4. Load function $q_{w,1}(z,\varphi)$.

Table 1
Comparison of results for current FEA and ABAQUS S4R shell FEA for example 4.

		Point *A*	Point *B*	Point *C*
Vertical Disp.	Current FEA	0.4022	0.4361	0.4688
	ABAQUS S4R element	0.4143	0.4491	0.4833
Lateral Disp.	Current FEA	0	0.03331	0
	ABAQUS S4R element	0	0.03453	0
Long. Disp.	Current FEA	-0.05109	-0.000672	0.04974
	ABAQUS S4R element	-0.05419	-0.00160	0.05099

The results in Table 1 show that the displacements predicted by the current method closely match those of the ABAQUS S4R shell finite element analysis (1296 nodes with 6 degrees of freedom per node). The current analysis is able to capture the axisymmetric radial expansion of the pipe induced by the internal pressure as well as the vertical displacement due to the self-weight of the pipe and the fluid.

5. Conclusions

1. A finite element solution was formulated based on the analytical solution developed in [1]. The displacement fields were interpolated using a series of exact shape functions which relate the intermediate displacements within a pipe finite element to the nodal displacements. Using the exact shape functions, the principle of stationary potential energy was adopted to formulate the "exact" stiffness matrices and associated energy equivalent load vectors for common loads. The new finite element was tested for a variety of practical loading conditions including point loads, gravity loads, internal pressure, twisting deformation, transverse deformations, and combinations thereof. Results were in excellent agreement with those based on shell finite elements in ABAQUS.
2. The pipe element developed was shown to be free of discretization errors, a direct result of adopting the exact shape functions in the formulation. More refined results within the element are obtained by using higher order harmonics. A main advantage of the new element, in comparison with the conventional shell FEA, is its computational efficiency. This is a direct outcome of the orthogonal properties of the Fourier terms.
3. The new element can very accurately predict the displacements and stresses of a pipe with just a single element between supports. Excellent displacement results are obtained using a few harmonics and accurate stress values were obtained using only seven harmonics. In comparison, conventional shell FEA would require a number of degrees of freedom a few orders of magnitudes higher to obtain results of comparable accuracy. The simplicity of the new element relative to a shell FEA also greatly reduces the modelling effort required by the analyst.
4. Another feature of the new element is its convergence characteristics. In conventional shell FEA solutions, accuracy of results is improved by refining the element mesh and repeating the analysis until convergence is achieved. In contrast, with the new pipe element, improved accuracy is achieved by including additional Fourier modes in the analysis. The results from the additional modes can simply be added to those of previous modes to obtain the total results. There is no need to repeat the analysis for previous modes.

Appendix A. Expressions for displacement fields

A.1. Displacement contribution for mode $n = 0$

With reference to [1], the displacement contributions for mode $n = 0$ are

$$\begin{aligned} a_0(z) &= \langle e_0(z)\rangle_{1\times 8}^{\mathrm{T}}\{\overline{A}_0\}_{8\times 1} \\ c_0(z) &= \langle \overline{\overline{C}}_0(z)\rangle_{1\times 8}^{\mathrm{T}}\{\overline{A}_0\}_{8\times 1} \\ f_0(z) &= \langle \overline{\overline{F}}_0(z)\rangle_{1\times 8}^{\mathrm{T}}\{\overline{A}_0\}_{8\times 1} \end{aligned} \quad \text{(A.1a –c)}$$

in which

$$\begin{aligned} \langle e_0(z)\rangle_{1\times 8}^{\mathrm{T}} &= \langle 1 \;\; z \;\; e^{m_{0,3}z} \;\; e^{m_{0,4}z} \;\; e^{m_{0,5}z} \;\; e^{m_{0,6}z} \;\; 0 \;\; 0\rangle \\ \langle \overline{\overline{C}}_0(z)\rangle_{1\times 8}^{\mathrm{T}} &= \langle 0 \;\; 0 \;\; 0 \;\; 0 \;\; 0 \;\; 0 \;\; 1 \;\; z\rangle \\ \langle \overline{\overline{F}}_0(z)\rangle_{1\times 8}^{\mathrm{T}} &= \langle 0 \;\; \overline{\overline{F}}_{0,1} \;\; \overline{\overline{F}}_{0,3}e^{m_{0,3}z} \;\; \overline{\overline{F}}_{0,4}e^{m_{0,4}z} \;\; \overline{\overline{F}}_{0,5}e^{m_{0,5}z} \;\; \overline{\overline{F}}_{0,6}e^{m_{0,6}z} \;\; 0 \;\; 0\rangle \end{aligned} \quad \text{(A.2a–i)}$$

where

$$\begin{aligned} m_{0,3} &= \sqrt[4]{\frac{C_3^2 - C_1C_2}{C_1C_6}}, \;\; m_{0,4} = -\sqrt[4]{\frac{C_3^2 - C_1C_2}{C_1C_6}}, \\ m_{0,5} &= \sqrt[4]{\frac{C_3^2 - C_1C_2}{C_1C_6}}i, \;\; m_{0,6} = -\sqrt[4]{\frac{C_3^2 - C_1C_2}{C_1C_6}}i \end{aligned} \quad \text{(A.3a – d)}$$

$$\begin{aligned} \overline{\overline{F}}_{0,1} &= -\frac{C_3}{C_2}, \;\; \overline{\overline{F}}_{0,3} = -\frac{C_1}{C_3}m_{0,3}, \;\; \overline{\overline{F}}_{0,4} = -\frac{C_1}{C_3}m_{0,4}, \\ \overline{\overline{F}}_{0,5} &= -\frac{C_1}{C_3}m_{0,5}, \;\; \overline{\overline{F}}_{0,6} = -\frac{C_1}{C_3}m_{0,6} \end{aligned} \quad \text{(A.4a – e)}$$

In the present and following sections (A.2) and (A.3), the constants below are defined:

$$\begin{aligned} C_1 &= \frac{Ert\pi}{1-\nu^2} \;\; C_2 = \frac{Et\pi}{r(1-\nu^2)}, \;\; C_3 = \frac{Et\nu\pi}{1-\nu^2}, \;\; C_4 = Grt\pi \\ C_5 &= Gt\pi \;\; C_6 = \frac{Ert^3\pi}{12(1-\nu^2)}, \;\; C_7 = \frac{Et^3\pi}{12r^3(1-\nu^2)}, \\ C_8 &= \frac{Et^3\nu\pi}{12r(1-\nu^2)}, \;\; C_9 = \frac{Gt^3\pi}{3r}, \;\; C_{10,n} = \frac{C_4n^2}{r^2}, \\ C_{11,n} &= (C_3 + C_5)n, \;\; C_{12,n} = (C_2 + C_7)n^2, \;\; C_{13} = C_4 + C_9, \\ C_{14,n} &= C_2n + C_7n^3, \;\; C_{15,n} = (C_8 + C_9)n, \;\; C_{16,n} = C_2 + C_7n^4 \\ C_{17,n} &= (2C_8 + C_9)n^2 \end{aligned} \quad \text{(A.5a – q)}$$

A.2. Displacement contribution for mode $n = 1$

The displacement contributions for mode $n = 1$ are:

$$\begin{aligned} a_1(z) &= \langle \overline{\overline{A}}_1(z)\rangle_{1\times 8}^{\mathrm{T}}\{\overline{F}_1\}_{8\times 1}, \;\; d_1(z) = \langle \overline{\overline{D}}_1(z)\rangle_{1\times 8}^{\mathrm{T}}\{\overline{F}_1\}_{8\times 1}, \\ f_1(z) &= \langle e_1(z)\rangle_{1\times 8}^{\mathrm{T}}\{\overline{F}_1\}_{8\times 1} \\ b_1(z) &= \langle \overline{\overline{A}}_1(z)\rangle_{1\times 8}^{\mathrm{T}}\{\overline{G}_1\}_{8\times 1}, \;\; c_1(z) = -\langle \overline{\overline{D}}_1(z)\rangle_{1\times 8}^{\mathrm{T}}\{\overline{G}_1\}_{8\times 1}, \\ g_1(z) &= \langle e_1(z)\rangle_{1\times 8}^{\mathrm{T}}\{\overline{G}_1\}_{8\times 1} \end{aligned} \quad \text{(A.6a – f)}$$

where

$$\begin{aligned} \langle e_1(z)\rangle_{1\times 8}^{\mathrm{T}} &= \langle 1 \;\; z \;\; z^2 \;\; z^3 \;\; e^{m_{1,5}z} \;\; e^{m_{1,6}z} \;\; e^{m_{1,7}z} \;\; e^{m_{1,8}z}\rangle_{1\times 8} \\ \langle \overline{\overline{A}}_1(z)\rangle_{1\times 8}^{\mathrm{T}} &= \langle 0 \;\; \overline{\overline{A}}_{1,1.1} \;\; \overline{\overline{A}}_{1,2}z \;\; (\overline{\overline{A}}_{1,1.2} + \overline{\overline{A}}_{1,3}z^2) \\ &\quad \overline{\overline{A}}_{1,5}e^{m_{1,5}z} \;\; \overline{\overline{A}}_{1,6}e^{m_{1,6}z} \;\; \overline{\overline{A}}_{1,7}e^{m_{1,7}z} \;\; \overline{\overline{A}}_{1,8}e^{m_{1,8}z}\rangle_{1\times 8} \\ \langle \overline{\overline{D}}_1(z)\rangle_{1\times 8}^{\mathrm{T}} &= \langle \overline{\overline{D}}_{1,1.1} \;\; \overline{\overline{D}}_{1,2.1}z \;\; (\overline{\overline{D}}_{1,1.2} + \overline{\overline{D}}_{1,3}z^2) \\ &\quad \left(\overline{\overline{D}}_{1,2.2}z + \overline{\overline{D}}_{1,4}z^3\right) \overline{\overline{D}}_{1,5}e^{m_{1,5}z} \;\; \overline{\overline{D}}_{1,6}e^{m_{1,6}z} \\ &\quad \overline{\overline{D}}_{1,7}e^{m_{1,7}z}\overline{\overline{D}}_{1,8}e^{m_{1,8}z}\rangle_{1\times 8} \end{aligned} \quad \text{(A.7a –c)}$$

and

$$m_{1,5} = \sqrt{\left(-p_{2,1}+\sqrt{p_{2,1}^2-4p_1p_{3,1}}\right)/2p_1},$$
$$m_{1,6} = -\sqrt{\left(-p_{2,1}+\sqrt{p_{2,1}^2-4p_1p_{3,1}}\right)/2p_1}$$
$$m_{1,7} = \sqrt{\left(-p_{2,1}-\sqrt{p_{2,1}^2-4p_1p_{3,1}}\right)/2p_1},$$
$$m_{1,8} = -\sqrt{\left(-p_{2,1}-\sqrt{p_{2,1}^2-4p_1p_{3,1}}\right)/2p_1} \qquad \text{(A.8a – d)}$$

in which

$$p_1 = -C_1C_6C_{13}$$
$$p_{2,1} = C_1\left(C_6C_{12,1}+C_{13}C_{17,1}-{C_{15,1}}^2\right)+C_6\left(C_{10,1}C_{13}-{C_{11,1}}^2\right)$$
$$p_{3,1} = C_1(-C_{12,1}C_{17,1}-C_{13}C_{16,1}+2C_{14,1}C_{15,1}) - C_{10,1}\left(C_6C_{12,1}+C_{13}C_{17,1}-{C_{15,1}}^2\right)+{C_{11,1}}^2C_{17,1} - 2C_3C_{11,1}C_{15,1}+C_3^2C_{13} \qquad \text{(A.9a – c)}$$

and

$$\overline{\overline{A}}_{1,1.1} = \frac{1}{C_{10,1}}\left(C_3-\frac{C_{11,1}C_{14,1}}{C_{12,1}}\right) \quad \overline{\overline{A}}_{1,2} = \frac{2}{C_{10,1}}\left(C_3-\frac{C_{11,1}C_{14,1}}{C_{12,1}}\right)$$
$$\overline{\overline{A}}_{1,1.2} = \frac{6C_1}{C_{10,1}^2}\left[-\frac{C_{11,1}C_{14,1}}{C_{12,1}}+C_3\right]+\frac{6C_{11,1}}{C_{10,1}C_{12,1}} \left[\frac{C_{11,1}}{C_{10,1}}\left(\frac{C_{11,1}C_{14,1}}{C_{12,1}}-C_3\right)-\frac{C_{13}C_{14,1}}{C_{12,1}}+C_{15,1}\right]$$
$$\overline{\overline{A}}_{1,3} = \frac{3}{C_{10}}\left(C_3-\frac{C_{11}C_{14}}{C_{12}}\right),$$

$$\overline{\overline{A}}_{1,i} = \frac{-\frac{(C_{11,1}m_{1,i})}{(C_1m_{1,i}^2-C_{10,1})}\left[\frac{(C_{11,1}m_{1,i})(C_3m_{1,i})}{(C_1m_1^2-C_{10,1})}-(C_{14,1}-C_{15,1}m_{1,i}^2)\right]}{\left(C_{12,1}-C_{13}{m_{1,i}}^2\right)-\frac{(C_{11,1}m_{1,i})^2}{(C_1m_{1,i}^2-C_{10,1})}} - \frac{(C_3m_{1,i})}{(C_1m_{1,i}^2-C_{10,1})}$$

$$\overline{\overline{D}}_{1,1.1} = -\frac{C_{14,1}}{C_{12,1}} \quad , \quad \overline{\overline{D}}_{1,2.1} = -\frac{C_{14,1}}{C_{12,1}},$$
$$\overline{\overline{D}}_{1,1.2} = \frac{2}{C_{12,1}}\left[\frac{C_{11,1}}{C_{10,1}}\left(\frac{C_{11,1}C_{14,1}}{C_{12,1}}-C_3\right)-\frac{C_{13}C_{14,1}}{C_{12,1}}+C_{15,1}\right]$$
$$\overline{\overline{D}}_{1,2.2} = \frac{6}{C_{12}}\left[\frac{C_{11,1}}{C_{10,1}}\left(\frac{C_{11,1}C_{14,1}}{C_{12,1}}-C_3\right)-\frac{C_{13}C_{14,1}}{C_{12,1}}+C_{15,1}\right],$$

$$\overline{\overline{D}}_{1,i} = \frac{\frac{(C_{11,1}m_{1,i})(C_3m_{1,i})}{(C_1m_{1,i}^2-C_{10,1})}-(C_{14,1}-C_{15,1}m_{1,i}^2)}{(C_{12,1}-C_{13}m_{1,i}^2)-\frac{(C_{11,1}m_{1,i})^2}{(C_1m_{1,i}^2-C_{10,1})}} \qquad \text{(A.10a – j)}$$

A.3. Displacement contribution for modes $n > 1$

The displacement contributions for mode $n > 1$ are

$$a_n(z) = \langle\overline{\overline{A}}_n(z)\rangle_{1\times8}^{\mathrm{T}}\{\overline{F}_n\}_{8\times1}, \quad d_n(z) = \langle\overline{\overline{D}}_n(z)\rangle_{1\times8}^{\mathrm{T}}\{\overline{F}_n\}_{8\times1},$$
$$f_n(z) = \langle e_n(z)\rangle_{1\times8}^{\mathrm{T}}\{\overline{F}_n\}_{8\times1}$$
$$b_n(z) = \langle\overline{\overline{A}}_n(z)\rangle_{1\times8}^{\mathrm{T}}\{\overline{G}_n\}_{8\times1}, \quad c_n(z) = -\langle\overline{\overline{D}}_n(z)\rangle_{1\times8}^{\mathrm{T}}\{\overline{G}_n\}_{8\times1},$$
$$g_n(z) = \langle e_n(z)\rangle_{1\times8}^{\mathrm{T}}\{\overline{G}_n\}_{8\times1} \qquad \text{(A.11a – f)}$$

$$\langle\overline{\overline{A}}_n(z)\rangle_{1\times8}^{\mathrm{T}} = \langle\overline{\overline{A}}_{n,1}e^{m_{n,1}z} \quad \overline{\overline{A}}_{n,2}e^{m_{n,2}z} \quad \overline{\overline{A}}_{n,3}e^{m_{n,3}z} \quad \overline{\overline{A}}_{n,4}e^{m_{n,4}z} \quad \overline{\overline{A}}_{n,5}e^{m_{n,5}z} \quad \overline{\overline{A}}_{n,6}e^{m_{n,6}z} \quad \overline{\overline{A}}_{n,7}e^{m_{n,7}z} \quad \overline{\overline{A}}_{n,8}e^{m_{n,8}z}\rangle_{1\times8}$$
$$\langle\overline{\overline{D}}_n(z)\rangle_{1\times8}^{\mathrm{T}} = \langle\overline{\overline{D}}_{n,1}e^{m_{n,1}z} \quad \overline{\overline{D}}_{n,2}e^{m_{n,2}z} \quad \overline{\overline{D}}_{n,3}e^{m_{n,3}z} \quad \overline{\overline{D}}_{n,4}e^{m_{n,4}z} \quad \overline{\overline{D}}_{n,5}e^{m_{n,5}z} \quad \overline{\overline{D}}_{n,6}e^{m_{n,6}z} \quad \overline{\overline{D}}_{n,7}e^{m_{n,7}z} \quad \overline{\overline{D}}_{n,8}e^{m_{n,8}z}\rangle_{1\times8}$$
$$\langle e_n(z)\rangle_{1\times8}^{\mathrm{T}} = \langle e^{m_{n,1}z} \quad e^{m_{n,2}z} \quad e^{m_{n,3}z} \quad e^{m_{n,4}z} \quad e^{m_{n,5}z} \quad e^{m_{n,6}z} \quad e^{m_{n,7}z}e^{m_{n,8}z}\rangle_{1\times8} \qquad \text{(A.12a –c)}$$

where $m_{n,i}$ $(i = 1,\ldots,8)$ are determined from

$$p_1 = -C_1C_6C_{13}$$
$$p_{2,n} = C_1\left(C_6C_{12,n}+C_{13}C_{17,n}-{C_{15,n}}^2\right)+C_6\left(C_{10,n}C_{13}-C_{11,n}^2\right)$$
$$p_{3,n} = C_1(-C_{12,n}C_{17,n}-C_{13}C_{16,n}+2C_{14,n}C_{15,n}) - C_{10,n}\left(C_6C_{12,n}+C_{13}C_{17,n}-C_{15,n}^2\right)+C_{11,n}^2C_{17,n} - 2C_3C_{11,n}C_{15,n}+C_3^2C_{13}$$
$$p_{4,n} = C_1\left(C_{12,n}C_{16,n}-C_{14,n}^2\right)+C_{10,n}(C_{12,n}C_{17,n}+C_{13}C_{16,n} - 2C_{14,n}C_{15,n})+2C_3C_{11,n}C_{14,n}-C_{11,n}^2C_{16,n}-C_3^2C_{12,n}$$
$$p_{5,n} = -C_{10,n}\left(C_{12,n}C_{16,n}-C_{14,n}^2\right) \qquad \text{(A.13a – e)}$$

The four complex roots $M_{n,1}$, $M_{n,2}$, $M_{n,3}$, and $M_{n,4}$ of the characteristic polynomial $p_1M_n^4+p_{2,n}M_n^3+p_{3,n}M_n^2+p_{4,n}M_n+p_{5,n} = 0$ are determined. All four roots are observed to be distinct when $n \geq 2$. The eight constants $m_{n,i}(i = 1\ldots8)$ are then determined from $m_{n,i} = \pm\sqrt{M_{n,j}}(j = 1\ldots4)$.

Appendix B. Matrices relating integration constant vectors to nodal displacement vectors

Mode $n = 0$

$$[L_0]_{8\times8} = \begin{bmatrix} 1 & 0 & 1 & 1 & 1 & 1 & 0 & 0 \\ 0 & 0 & 0 & 0 & 0 & 0 & 1 & 0 \\ 0 & \overline{\overline{F}}_{0,1} & \overline{\overline{F}}_{0,3} & \overline{\overline{F}}_{0,4} & \overline{\overline{F}}_{0,5} & \overline{\overline{F}}_{0,6} & 0 & 0 \\ 0 & 0 & m_{0,3}\overline{\overline{F}}_{0,3} & m_{0,4}\overline{\overline{F}}_{0,4} & m_{0,5}\overline{\overline{F}}_{0,5} & m_{0,6}\overline{\overline{F}}_{0,6} & 0 & 0 \\ 1 & \ell & e^{m_{0,3}\ell} & e^{m_{0,4}\ell} & e^{m_{0,5}\ell} & e^{m_{0,6}\ell} & 0 & 0 \\ 0 & 0 & 0 & 0 & 0 & 0 & 1 & \ell \\ 0 & \overline{\overline{F}}_{0,1} & \overline{\overline{F}}_{0,3}e^{m_{0,3}\ell} & \overline{\overline{F}}_{0,4}e^{m_{0,4}\ell} & \overline{\overline{F}}_{0,5}e^{m_{0,5}\ell} & \overline{\overline{F}}_{0,6}e^{m_{0,6}\ell} & 0 & 0 \\ 0 & 0 & m_{0,3}\overline{\overline{F}}_{0,3}e^{m_{0,3}\ell} & m_{0,4}\overline{\overline{F}}_{0,4}e^{m_{0,4}\ell} & m_{0,5}\overline{\overline{F}}_{0,5}e^{m_{0,5}\ell} & m_{0,6}\overline{\overline{F}}_{0,6}e^{m_{0,6}\ell} & 0 & 0 \end{bmatrix} \qquad \text{(B.1)}$$

Mode $n=1$

$$[L_{1,1}]_{8\times 8}=\begin{bmatrix}
0 & \overline{\overline{A}}_{1,1.1} & 0 & \overline{\overline{A}}_{1,1.2} & \overline{\overline{A}}_{1,5} & \overline{\overline{A}}_{1,6} & \overline{\overline{A}}_{1,7} & \overline{\overline{A}}_{1,8}\\
\overline{\overline{D}}_{1,1.1} & 0 & \overline{\overline{D}}_{1,1.2} & 0 & \overline{\overline{D}}_{1,5} & \overline{\overline{D}}_{1,6} & \overline{\overline{D}}_{1,7} & \overline{\overline{D}}_{1,8}\\
1 & 0 & 0 & 0 & 1 & 1 & 1 & 1\\
0 & 1 & 0 & 0 & m_{1,5} & m_{1,6} & m_{1,7} & m_{1,8}\\
0 & \overline{\overline{A}}_{1,1.1} & \overline{\overline{A}}_{1,2}\ell & \overline{\overline{A}}_{1,1.2}+\overline{\overline{A}}_{1,3}\ell^2 & \overline{\overline{A}}_{1,5}e^{m_{1,5}\ell} & \overline{\overline{A}}_{1,6}e^{m_{1,6}\ell} & \overline{\overline{A}}_{1,7}e^{m_{1,7}\ell} & \overline{\overline{A}}_{1,8}e^{m_{1,8}\ell}\\
\overline{\overline{D}}_{1,1.1} & \overline{\overline{D}}_{1,2.1}\ell & \overline{\overline{D}}_{1,1.2}+\overline{\overline{D}}_{1,3}\ell^2 & \overline{\overline{D}}_{1,2.2}\ell+\overline{\overline{D}}_{1,4}\ell^3 & \overline{\overline{D}}_{1,5}e^{m_{1,5}\ell} & \overline{\overline{D}}_{1,6}e^{m_{1,6}\ell} & \overline{\overline{D}}_{1,7}e^{m_{1,7}\ell} & \overline{\overline{D}}_{1,8}e^{m_{1,8}\ell}\\
1 & \ell & \ell^2 & \ell^3 & e^{m_{1,5}\ell} & e^{m_{1,6}\ell} & e^{m_{1,7}\ell} & e^{m_{1,8}\ell}\\
0 & 1 & 2\ell & 3\ell^2 & m_{1,5}e^{m_{1,5}\ell} & m_{1,6}e^{m_{1,6}\ell} & m_{1,7}e^{m_{1,7}\ell} & m_{1,8}e^{m_{1,8}\ell}
\end{bmatrix}$$

$$[L_{1,2}]_{8\times 8}=\begin{bmatrix}
0 & \overline{\overline{A}}_{1,1.1} & 0 & \overline{\overline{A}}_{1,1.2} & \overline{\overline{A}}_{1,5} & \overline{\overline{A}}_{1,6} & \overline{\overline{A}}_{1,7} & \overline{\overline{A}}_{1,8}\\
-\overline{\overline{D}}_{1,1.1} & 0 & -\overline{\overline{D}}_{1,1.2} & 0 & -\overline{\overline{D}}_{1,5} & -\overline{\overline{D}}_{1,6} & -\overline{\overline{D}}_{1,7} & -\overline{\overline{D}}_{1,8}\\
1 & 0 & 0 & 0 & 1 & 1 & 1 & 1\\
0 & 1 & 0 & 0 & m_{1,5} & m_{1,6} & m_{1,7} & m_{1,8}\\
0 & \overline{\overline{A}}_{1,1.1} & \overline{\overline{A}}_{1,2}\ell & \overline{\overline{A}}_{1,1.2}+\overline{\overline{A}}_{1,3}\ell^2 & \overline{\overline{A}}_{1,5}e^{m_{1,5}\ell} & \overline{\overline{A}}_{1,6}e^{m_{1,6}\ell} & \overline{\overline{A}}_{1,7}e^{m_{1,7}\ell} & \overline{\overline{A}}_{1,8}e^{m_{1,8}\ell}\\
-\overline{\overline{D}}_{1,1.1} & -\overline{\overline{D}}_{1,2.1}\ell & -\overline{\overline{D}}_{1,1.2}-\overline{\overline{D}}_{1,3}\ell^2 & -\overline{\overline{D}}_{1,2.2}\ell-\overline{\overline{D}}_{1,4}\ell^3 & -\overline{\overline{D}}_{1,5}e^{m_{1,5}\ell} & -\overline{\overline{D}}_{1,6}e^{m_{1,6}\ell} & -\overline{\overline{D}}_{1,7}e^{m_{1,7}\ell} & -\overline{\overline{D}}_{1,8}e^{m_{1,8}\ell}\\
1 & \ell & \ell^2 & \ell^3 & e^{m_{1,5}\ell} & e^{m_{1,6}\ell} & e^{m_{1,7}\ell} & e^{m_{1,8}\ell}\\
0 & 1 & 2\ell & 3\ell^2 & m_{1,5}e^{m_{1,5}\ell} & m_{1,6}e^{m_{1,6}\ell} & m_{1,7}e^{m_{1,7}\ell} & m_{1,8}e^{m_{1,8}\ell}
\end{bmatrix} \qquad \text{(B.2a – b)}$$

Modes $n\geq 2$

$$[L_{n,1}]_{8\times 8}=\begin{bmatrix}
\overline{\overline{A}}_{n,1} & \overline{\overline{A}}_{n,2} & \overline{\overline{A}}_{n,3} & \overline{\overline{A}}_{n,4} & \overline{\overline{A}}_{n,5} & \overline{\overline{A}}_{n,6} & \overline{\overline{A}}_{n,7} & \overline{\overline{A}}_{n,8}\\
\overline{\overline{D}}_{n,1} & \overline{\overline{D}}_{n,2} & \overline{\overline{D}}_{n,3} & \overline{\overline{D}}_{n,4} & \overline{\overline{D}}_{n,5} & \overline{\overline{D}}_{n,6} & \overline{\overline{D}}_{n,7} & \overline{\overline{D}}_{n,8}\\
1 & 1 & 1 & 1 & 1 & 1 & 1 & 1\\
m_{n,1} & m_{n,2} & m_{n,3} & m_{n,4} & m_{n,5} & m_{n,6} & m_{n,7} & m_{n,8}\\
\overline{\overline{A}}_{n,1}e^{m_{n,1}\ell} & \overline{\overline{A}}_{n,2}e^{m_{n,2}\ell} & \overline{\overline{A}}_{n,3}e^{m_{n,3}\ell} & \overline{\overline{A}}_{n,4}e^{m_{n,4}\ell} & \overline{\overline{A}}_{n,5}e^{m_{n,5}\ell} & \overline{\overline{A}}_{n,6}e^{m_{n,6}\ell} & \overline{\overline{A}}_{n,7}e^{m_{n,7}\ell} & \overline{\overline{A}}_{n,8}e^{m_{n,8}\ell}\\
\overline{\overline{D}}_{n,1}e^{m_{n,1}\ell} & \overline{\overline{D}}_{n,2}e^{m_{n,2}\ell} & \overline{\overline{D}}_{n,3}e^{m_{n,3}\ell} & \overline{\overline{D}}_{n,4}e^{m_{n,4}\ell} & \overline{\overline{D}}_{n,5}e^{m_{n,5}\ell} & \overline{\overline{D}}_{n,6}e^{m_{n,6}\ell} & \overline{\overline{D}}_{n,7}e^{m_{n,7}\ell} & \overline{\overline{D}}_{n,8}e^{m_{n,8}\ell}\\
e^{m_{n,1}\ell} & e^{m_{n,2}\ell} & e^{m_{n,3}\ell} & e^{m_{n,4}\ell} & e^{m_{n,5}\ell} & e^{m_{n,6}\ell} & e^{m_{n,7}\ell} & e^{m_{n,8}\ell}\\
m_{n,1}e^{m_{n,1}\ell} & m_{n,2}e^{m_{n,2}\ell} & m_{n,3}e^{m_{n,3}\ell} & m_{n,4}e^{m_{n,4}\ell} & m_{n,5}e^{m_{n,5}\ell} & m_{n,6}e^{m_{n,6}\ell} & m_{n,7}e^{m_{n,7}\ell} & m_{n,8}e^{m_{n,8}\ell}
\end{bmatrix}$$

$$[L_{n,2}]_{8\times 8}=\begin{bmatrix}
\overline{\overline{A}}_{n,1} & \overline{\overline{A}}_{n,2} & \overline{\overline{A}}_{n,3} & \overline{\overline{A}}_{n,4} & \overline{\overline{A}}_{n,5} & \overline{\overline{A}}_{n,6} & \overline{\overline{A}}_{n,7} & \overline{\overline{A}}_{n,8}\\
-\overline{\overline{D}}_{n,1} & -\overline{\overline{D}}_{n,2} & -\overline{\overline{D}}_{n,3} & -\overline{\overline{D}}_{n,4} & -\overline{\overline{D}}_{n,5} & -\overline{\overline{D}}_{n,6} & -\overline{\overline{D}}_{n,7} & -\overline{\overline{D}}_{n,8}\\
1 & 1 & 1 & 1 & 1 & 1 & 1 & 1\\
m_{n,1} & m_{n,2} & m_{n,3} & m_{n,4} & m_{n,5} & m_{n,6} & m_{n,7} & m_{n,8}\\
\overline{\overline{A}}_{n,1}e^{m_{n,1}\ell} & \overline{\overline{A}}_{n,2}e^{m_{n,2}\ell} & \overline{\overline{A}}_{n,3}e^{m_{n,3}\ell} & \overline{\overline{A}}_{n,4}e^{m_{n,4}\ell} & \overline{\overline{A}}_{n,5}e^{m_{n,5}\ell} & \overline{\overline{A}}_{n,6}e^{m_{n,6}\ell} & \overline{\overline{A}}_{n,7}e^{m_{n,7}\ell} & \overline{\overline{A}}_{n,8}e^{m_{n,8}\ell}\\
-\overline{\overline{D}}_{n,1}e^{m_{n,1}\ell} & -\overline{\overline{D}}_{n,2}e^{m_{n,2}\ell} & -\overline{\overline{D}}_{n,3}e^{m_{n,3}\ell} & -\overline{\overline{D}}_{n,4}e^{m_{n,4}\ell} & -\overline{\overline{D}}_{n,5}e^{m_{n,5}\ell} & -\overline{\overline{D}}_{n,6}e^{m_{n,6}\ell} & -\overline{\overline{D}}_{n,7}e^{m_{n,7}\ell} & -\overline{\overline{D}}_{n,8}e^{m_{n,8}\ell}\\
e^{m_{n,1}\ell} & e^{m_{n,2}\ell} & e^{m_{n,3}\ell} & e^{m_{n,4}\ell} & e^{m_{n,5}\ell} & e^{m_{n,6}\ell} & e^{m_{n,7}\ell} & e^{m_{n,8}\ell}\\
m_{n,1}e^{m_{n,1}\ell} & m_{n,2}e^{m_{n,2}\ell} & m_{n,3}e^{m_{n,3}\ell} & m_{n,4}e^{m_{n,4}\ell} & m_{n,5}e^{m_{n,5}\ell} & m_{n,6}e^{m_{n,6}\ell} & m_{n,7}e^{m_{n,7}\ell} & m_{n,8}e^{m_{n,8}\ell}
\end{bmatrix} \qquad \text{(B.3a – b)}$$

Appendix C. Components of stiffness matrices and load vectors

$$\begin{aligned}[K_0]_{8\times 8}=\int_{z=0}^{l} & 2C_1\{N'_{A,0}(z)\}_{8\times 1}\langle N'_{A,0}(z)\rangle^{\mathrm{T}}_{1\times 8}+2C_2\{N_{F,0}(z)\}_{8\times 1}\langle N_{F,0}(z)\rangle^{\mathrm{T}}_{1\times 8}+2C_3\Big(\{N'_{A,0}(z)\}_{8\times 1}\langle N_{F,0}(z)\rangle^{\mathrm{T}}_{1\times 8}\\
&+\{N_{F,0}(z)\}_{8\times 1}\langle N'_{A,0}(z)\rangle^{\mathrm{T}}_{1\times 8}\Big)+2C_4\Big(\{N'_{C,0}(z)\}_{8\times 1}\langle N'_{C,0}(z)\rangle^{\mathrm{T}}_{1\times 8}\Big)+2C_6\Big(\{N''_{F,0}(z)\}_{8\times 1}\langle N''_{F,0}(z)\rangle^{\mathrm{T}}_{1\times 8}\Big)\\
&+2C_9\Big(\{N'_{C,0}(z)\}_{8\times 1}\langle N'_{C,0}(z)\rangle^{\mathrm{T}}_{1\times 8}\Big)dz \qquad \text{(C.1)}\end{aligned}$$

$$[K_{n,1}]_{8\times8} = \int_{z=0}^{l} C_1\{N'_{A,n}(z)\}_{8\times1}\langle N'_{A,n}(z)\rangle^{\mathrm{T}}_{1\times8}dz + \int_{z=0}^{l} C_2\Big[\{N_{F,n}(z)\}_{8\times1}\langle N_{F,n}(z)\rangle^{\mathrm{T}}_{1\times8} + n\Big(\{N_{D,n}(z)\}_{8\times1}\langle N_{F,n}(z)\rangle^{\mathrm{T}}_{1\times8} + \{N_{F,n}(z)\}_{8\times1}$$
$$\langle N_{D,n}(z)\rangle^{\mathrm{T}}_{1\times8}\Big) + n^2\{N_{D,n}(z)\}_{8\times1}\langle N_{D,n}(z)\rangle^{\mathrm{T}}_{1\times8}\Big]dz + \int_{z=0}^{l} C_3\Big[\{N'_{A,n}(z)\}_{8\times1}\langle N_{F,n}(z)\rangle^{\mathrm{T}}_{1\times8} + \{N_{F,n}(z)\}_{8\times1}\langle N'_{A,n}(z)\rangle^{\mathrm{T}}_{1\times8}$$
$$+ n\Big(\{N'_{A,n}(z)\}_{8\times1}\langle N_{D,n}(z)\rangle^{\mathrm{T}}_{1\times8} + \{N_{D,n}(z)\}_{8\times1}\langle N'_{A,n}(z)\rangle^{\mathrm{T}}_{1\times8}\Big)\Big]dz + \int_{z=0}^{l}\Big[C_4\{N'_{D,n}(z)\}_{8\times1}\langle N'_{D,n}(z)\rangle^{\mathrm{T}}_{1\times8} - C_5n\Big(\{N_{A,n}(z)\}_{8\times1}$$
$$\langle N'_{D,n}(z)\rangle^{\mathrm{T}}_{1\times8} + \{N'_{D,n}(z)\}_{8\times1}\langle N_{A,n}(z)\rangle^{\mathrm{T}}_{1\times8}\Big) + \frac{C_4n^2}{r^2}\{N_{A,n}(z)\}_{8\times1}\langle N_{A,n}(z)\rangle^{\mathrm{T}}_{1\times8}\Big]dz + \int_{z=0}^{l} C_6\{N''_{F,n}(z)\}_{8\times1}\langle N''_{F,n}(z)\rangle^{\mathrm{T}}_{1\times8}dz$$
$$+ \int_{z=0}^{l} C_7\Big[n^4\{N_{F,n}(z)\}_{8\times1}\langle N_{F,n}(z)\rangle^{\mathrm{T}}_{1\times8} + n^3\Big(\{N_{D,n}(z)\}_{8\times1}\langle N_{F,n}(z)\rangle^{\mathrm{T}}_{1\times8} + \{N_{F,n}(z)\}_{8\times1}\langle N_{D,n}(z)\rangle^{\mathrm{T}}_{1\times8}\Big) + n^2\{N_{D,n}(z)\}_{8\times1}$$
$$\langle N_{D,n}(z)\rangle^{\mathrm{T}}_{1\times8}\Big]dz + \int_{z=0}^{l} C_8\Big[-n^2\Big(\{N''_{F,n}(z)\}_{8\times1}\langle N_{F,n}(z)\rangle^{\mathrm{T}}_{1\times8} + \{N_{F,n}(z)\}_{8\times1}\langle N''_{F,n}(z)\rangle^{\mathrm{T}}_{1\times8}\Big) - n\Big(\{N_{D,n}(z)\}_{8\times1}\langle N''_{F,n}(z)\rangle^{\mathrm{T}}_{1\times8}$$
$$+ \{N''_{F,n}(z)\}_{8\times1}\langle N_{D,n}(z)\rangle^{\mathrm{T}}_{1\times8}\Big)\Big]dz + \int_{z=0}^{l} C_9\Big[n^2\{N'_{F,n}(z)\}_{16\times1}\langle N'_{F,n}(z)\rangle^{\mathrm{T}}_{1\times16} + n\Big(\{N'_{D,n}(z)\}_{16\times1}\langle N'_{F,n}(z)\rangle^{\mathrm{T}}_{1\times16}$$
$$+ \{N'_{F,n}(z)\}_{16\times1}\langle N'_{D,n}(z)\rangle^{\mathrm{T}}_{1\times16}\Big) + \{N'_{D,n}(z)\}_{16\times1}\langle N'_{D,n}(z)\rangle^{\mathrm{T}}_{1\times16}\Big]dz \tag{C.2}$$

$$[K_{n,2}]_{8\times8} = \int_{z=0}^{l} C_1\{N'_{B,n}(z)\}_{8\times1}\langle N'_{B,n}(z)\rangle^{\mathrm{T}}_{1\times8}dz + \int_{z=0}^{l} C_2\Big[\{N_{G,n}(z)\}_{8\times1}\langle N_{G,n}(z)\rangle^{\mathrm{T}}_{1\times8} - n\Big(\{N_{C,n}(z)\}_{8\times1}\langle N_{G,n}(z)\rangle^{\mathrm{T}}_{1\times8} + \{N_{G,n}(z)\}_{8\times1}$$
$$\langle N_{C,n}(z)\rangle^{\mathrm{T}}_{1\times8}\Big) + n^2\{N_{C,n}(z)\}_{8\times1}\langle N_{C,n}(z)\rangle^{\mathrm{T}}_{1\times8}\Big]dz + \int_{z=0}^{l}\Big[C_4\{N'_{C,n}(z)\}_{8\times1}\langle N'_{C,n}(z)\rangle^{\mathrm{T}}_{1\times8} + C_5n\Big(\{N_{B,n}(z)\}_{8\times1}\langle N'_{C,n}(z)\rangle^{\mathrm{T}}_{1\times8}$$
$$+ \{N'_{C,n}(z)\}_{8\times1}\langle N_{B,n}(z)\rangle^{\mathrm{T}}_{1\times8}\Big) + \frac{C_4n^2}{r^2}\{N_{B,n}(z)\}_{8\times1}\langle N_{B,n}(z)\rangle^{\mathrm{T}}_{1\times8}\Big]\mathrm{d}z + \int_{z=0}^{l} C_3\Big[\{N'_{B,n}(z)\}_{8\times1}\langle N_{G,n}(z)\rangle^{\mathrm{T}}_{1\times8} + \{N_{G,n}(z)\}_{8\times1}$$
$$\langle N'_{B,n}(z)\rangle^{\mathrm{T}}_{1\times8} - n\Big(\{N'_{B,n}(z)\}_{8\times1}\langle N_{C,n}(z)\rangle^{\mathrm{T}}_{1\times8} + \{N_{C,n}(z)\}_{8\times1}\langle N'_{B,n}(z)\rangle^{\mathrm{T}}_{1\times8}\Big)\Big]dz + \int_{z=0}^{l} C_6\{N''_{G,n}(z)\}_{8\times1}\langle N''_{G,n}(z)\rangle^{\mathrm{T}}_{1\times8}dz$$
$$+ \int_{z=0}^{l} C_7\Big[n^4\{N_{G,n}(z)\}_{8\times1}\langle N_{G,n}(z)\rangle^{\mathrm{T}}_{1\times8} - n^3\Big(\{N_{C,n}(z)\}_{8\times1}\langle N_{G,n}(z)\rangle^{\mathrm{T}}_{1\times8} + \{N_{G,n}(z)\}_{8\times1}\langle N_{C,n}(z)\rangle^{\mathrm{T}}_{1\times8}\Big) + n^2\{N_{C,n}(z)\}_{8\times1}$$
$$\langle N_{C,n}(z)\rangle^{\mathrm{T}}_{1\times8}\Big]dz + \int_{z=0}^{l} C_8\Big[-n^2\Big(\{N''_{G,n}(z)\}_{8\times1}\langle N_{G,n}(z)\rangle^{\mathrm{T}}_{1\times8} + \{N_{G,n}(z)\}_{8\times1}\langle N''_{G,n}(z)\rangle^{\mathrm{T}}_{1\times8}\Big) + n\Big(\{N_{C,n}(z)\}_{8\times1}\langle N''_{G,n}(z)\rangle^{\mathrm{T}}_{1\times8}$$
$$+ \{N''_{G,n}(z)\}_{8\times1}\langle N_{C,n}(z)\rangle^{\mathrm{T}}_{1\times8}\Big)\Big]\mathrm{d}z + \int_{z=0}^{l} C_9\Big[n^2\{N'_{G,n}(z)\}_{16\times1}\langle N'_{G,n}(z)\rangle^{\mathrm{T}}_{1\times16} - n\Big(\{N'_{C,n}(z)\}_{16\times1}\langle N'_{G,n}(z)\rangle^{\mathrm{T}}_{1\times16}$$
$$+ \{N'_{G,n}(z)\}_{16\times1}\langle N'_{C,n}(z)\rangle^{\mathrm{T}}_{1\times16}\Big) + \{N'_{C,n}(z)\}_{16\times1}\langle N'_{C,n}(z)\rangle^{\mathrm{T}}_{1\times16}\Big]\mathrm{d}z \tag{C.3}$$

$$\{Q_0\}_{8\times1} = \int_{z=0}^{\ell}\int_{\phi=0}^{2\pi}\Big[q_u(z,\phi)\{N_{A,0}(z)\}_{8\times1} + q_v(z,\phi)\{N_{C,0}(z)\}_{8\times1} + q_w(z,\phi)\{N_{F,0}(z)\}_{8\times1}\Big]r\mathrm{d}\phi\mathrm{d}z \tag{C.4}$$

$$\{Q_{n,1}\}_{8\times1} = \int_{z=0}^{\ell}\int_{\phi=0}^{2\pi}\Big[q_u(z,\phi)\{N_{A,n}(z)\}_{8\times1}\cos(n\phi) + q_v(z,\phi)\{N_{D,n}(z)\}_{8\times1}\sin(n\phi) + q_w(z,\phi)\{N_{F,n}(z)\}_{8\times1}\cos(n\phi)\Big]r\mathrm{d}\phi\mathrm{d}z \tag{C.5}$$

$$\{Q_{n,2}\}_{8\times1} = \int_{z=0}^{\ell}\int_{\phi=0}^{2\pi}\Big[q_u(z,\phi)\{N_{B,n}(z)\}_{8\times1}\sin(n\phi) + q_v(z,\phi)\{N_{C,n}(z)\}_{8\times1}\cos(n\phi) + q_w(z,\phi)\{N_{G,n}(z)\}_{8\times1}\sin(n\phi)\Big]r\mathrm{d}\phi\mathrm{d}z \tag{C.6}$$

References

[1] Weicker K, Salahifar R, Mohareb M. Shell analysis of thin-walled pipes – I. Field equations and solution. Int J Press Vessels Piping 2010;87:402–13.
[2] Mackerle J. Finite elements in the analysis of pressure vessels and piping – a bibliography (1976–1996). Int J Press Vessels Piping 1996;69:279–339.
[3] Mackerle J. Finite elements in the analysis of pressure vessels and piping, an addendum (1996–1998). Int J Press Vessels Piping 1999;76:461–85.
[4] Mackerle J. Finite elements in the analysis of pressure vessels and piping, an addendum: a bibliography (1998–2001). Int J Press Vessels Piping 2002;79: 1–26.
[5] Mackerle J. Finite elements in the analysis of pressure vessels and piping, an addendum: a bibliography (2001–2004). Int J Press Vessels Piping 2005;82: 571–92.
[6] Ohtsubo H, Watanabe O. Stress analysis of pipe bends by ring elements. J Press Vessel Technol 1978;100:112–22.
[7] Bathe KJ, Almeida C. A simple and effective pipe elbow element – linear analysis. J Appl Mech 1980;47:93–100.
[8] Bathe KJ, Almeida C. A simple and effective pipe elbow element – interaction effects. J Appl Mech 1982;49:165–71.
[9] Bathe KJ, Almeida C. A simple and effective pipe elbow element – some nonlinear capabilities. Comput Struct 1983;17:659–67.
[10] Militello C, Huespe AE. A displacement-based pipe elbow element. Comput Struct 1988;29(No. 2):339–43.
[11] Abo-Elkhier M. Analysis of pipe bends using pipe elbow element. Comput Struct 1990;37(No. 1):9–15.
[12] Yan AM, Jospin RJ, Nguyen DH. An enhanced pipe elbow element – application in plastic limit analysis of pipe structures. Int J Numer Methods Eng 1999;46(No. 3):409–31.
[13] Karamanos SA. Bending instabilities of elastic tubes. Int J Solids Struct 2002;39 (No. 8):2059–85.
[14] Karamanos SA, Giakoumatos E, Gresnigt AM. Nonlinear response and failure of steel elbows under in-plane bending and pressure. J Press Vessel Technol 2003;125(No. 4):393–402.
[15] Weicker, K. Finite element formulation for analysis of pipes based thin shell theory. M.A. Sc. thesis, Department of Civil Engineering, University of Ottawa, Ottawa, ON, Canada; 2008.

List of symbols

α: total number of terms included in the Fourier expansion,
$\{\Delta_0\}_{8\times1}$: nodal displacement vector corresponding to Fourier mode $n=0$,
$\{\Delta_{n,1}\}_{8\times1}$: nodal displacement vector corresponding for Fourier mode $n\geq1$ corresponding to displacements a_n, d_n and f_n,
$\{\Delta_{n,2}\}_{8\times1}$: nodal displacement vector corresponding for Fourier mode $n\geq1$ corresponding to displacements b_n, c_n and g_n,
$\{\overline{\Delta}_{n,1}\}_{2\times1}$: nodal displacement vector using linear interpolation shape functions,
ϵ_ϕ: total normal strain in the tangential direction,
$\overline{\epsilon}_\phi$: direct (membrane) strain in the tangential direction,
ϵ_z: total normal strain in the axial direction,
$\overline{\epsilon}_z$: direct (membrane) strain in the axial direction,
γ_s: density of steel pipe,
γ_w: density of water,
κ_φ: curvature in the tangential direction,
κ_z: curvature in the axial direction,
σ_z: normal stress in the axial direction,
$\prod^*$: total potential energy,
ν: Poisson's ratio,
ϕ: polar coordinate in the tangential direction,
ξ: material coordinate in the radial direction. The range of ξ is $-t/2$ to $+t/2$,
a_n, d_n, f_n, b_n, c_n, g_n: Functions of z only for mode n of the Fourier expansion of the displacements,
ℓ: length of the pipe or pipe element,
n: Fourier mode under consideration,
M_n,m_n: roots to the determinant of the operator matrix of the field equations ($M_n = m_n^2$),
p_1, p_2, p_3, p_4, p_5: coefficients of the 4th order (quartic) polynomial equation resulting from the determinant of the operator matrix of the field equations,
$q_u(z,\phi)$: applied tractions in the longitudinal direction,
$q_v(z,\phi)$: applied tractions in the tangential direction,
$q_w(z,\phi)$: applied tractions in the radial direction,
r: radius of the middle surface of the pipe cross section,
t: pipe wall thickness,
$u(z,\phi)$: total displacement in the longitudinal direction,
$v(z,\phi)$: total displacement in the tangential direction,
$w(z,\phi)$: total displacement in the radial direction,
z: coordinate in the longitudinal direction,
A: area of the pipe middle surface ($A = 2\pi r\ell$),
$\overline{A}_n, \overline{B}_n, \overline{C}_n, \overline{D}_n, \overline{F}_n, \overline{G}_n$: integration constants in the assumed displacement field corresponding to Fourier mode n,
$\overline{\overline{A}}_n, \overline{\overline{D}}_n$: constants relating $\overline{A}_n$ and $\overline{D}_n$, respectively, to $\overline{F}_n$,
$\overline{\overline{B}}_n, \overline{\overline{C}}_n$: constants relating $\overline{B}_n$ and $\overline{C}_n$, respectively, to $\overline{G}_n$,
$C_{1,2\ldots17}$: constants based on the geometric and material properties of the pipe as well as the Fourier mode n under consideration,
E: Young's modulus,
G: shear modulus,
$[K_{j,0}]_{8\times8}$: contribution to the total stiffness matrix for mode $n=0$ of term j (for $j=1$–8) of the total internal strain energy equation,
$[K_0]_{8\times8}$: total stiffness matrix for mode $n=0$,
$[K_{j,n,1}]_{8\times8}$: contribution to the total stiffness matrix corresponding to nodal displacements $\{\Delta_{n,1}\}_{8\times1}$ for mode $n\geq1$ of term j (for $j=1$–8) of the total internal strain energy equation,
$[K_{n,1}]_{8\times8}$: total stiffness matrix corresponding to nodal displacements $\{\Delta_{n,1}\}_{8\times1}$ for mode $n\geq1$,
$[K_{j,n,2}]_{8\times8}$: contribution to the total stiffness matrix corresponding to nodal displacements $\{\Delta_{n,2}\}_{8\times1}$ for mode $n\geq1$ of term j (for $j=1$–8) of the total internal strain energy equation,
$[K_{n,2}]_{8\times8}$: total stiffness matrix corresponding to nodal displacements $\{\Delta_{n,2}\}_{8\times1}$ for mode $n\geq1$,
$[L_0]_{8\times8}$: matrix relating the vector of integration constants $\{\overline{A}_0\}_{8\times1}$ to nodal displacements $\{\Delta_0\}_{8\times1}$ for mode $n=0$,
$[L_{1,1}]_{8\times8}$: matrix relating the vector of integration constants $\{\overline{F}_1\}_{8\times1}$ to nodal displacements $\{\Delta_{1,1}\}_{8\times1}$ for mode $n=1$,
$[L_{n,1}]_{8\times8}$: matrix relating the vector of integration constants $\{\overline{F}_n\}_{8\times1}$ to nodal displacements $\{\Delta_{n,1}\}_{8\times1}$ for mode $n\geq2$,
$[L_{1,2}]_{8\times8}$: matrix relating the vector of integration constants $\{\overline{G}_1\}_{8\times1}$ to nodal displacements $\{\Delta_{1,2}\}_{8\times1}$ for mode $n=1$,
$[L_{n,2}]_{8\times8}$: matrix relating the vector of integration constants $\{\overline{G}_n\}_{8\times1}$ to nodal displacements $\{\Delta_{n,2}\}_{8\times1}$ for mode $n\geq2$,
$\langle N_{X,n}(z)\rangle^T_{1\times8}$: exact shape function vectors for the displacements corresponding to Fourier mode n,
$\langle N(z)\rangle^T_{1\times2}$: linear interpolation shape function,
$\{Q_n\}_{8\times1}$: load potential vector,
U: Internal strain energy and
V: volume of the pipe element ($V = At = 2\pi r\ell t$).